# Lightweight, Durable, and Multifunctional Electrical Insulation Material Systems for High Voltage Applications

**E. Eugene Shin[1], Daniel A. Scheiman[1], and Maricela Lizcano[2]**

[1]Ohio Aerospace Institute, [2]NASA-GRC

**AIAA/IEEE Electric Aircraft Technologies Symposium (EATS)**
12 - 13 July, 2018, Cincinnati, Ohio

# Table of Contents

- **Backgrounds and Objectives**

- **Experimental**
  - Materials
  - Fabrication of Dielectric Strength Test Samples
  - Dielectric Strength Testing

- **Results and Discussion**
  - Status of the Invention
  - Design and Process Optimizations
  - Commercial Benefit/Applicability
    - High Voltage Power Cable
    - High Voltage High Frequency Bus Bar

- **Summary and Conclusions**

- **Future Work Plan**

- Potential Electric Propulsion Architectures by J.L. Felder, NASA-GRC
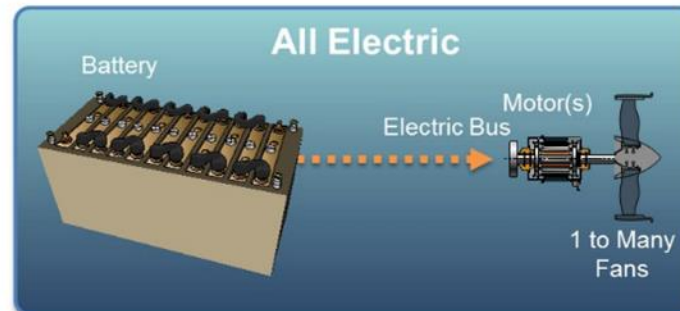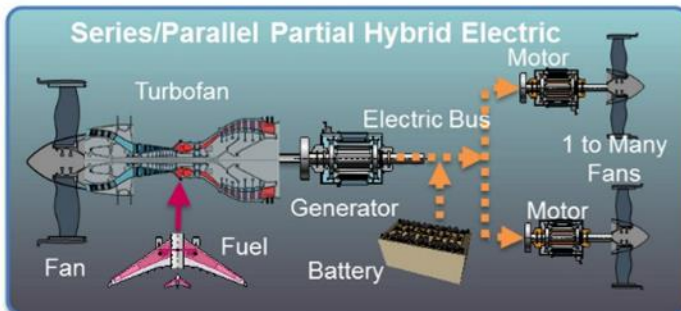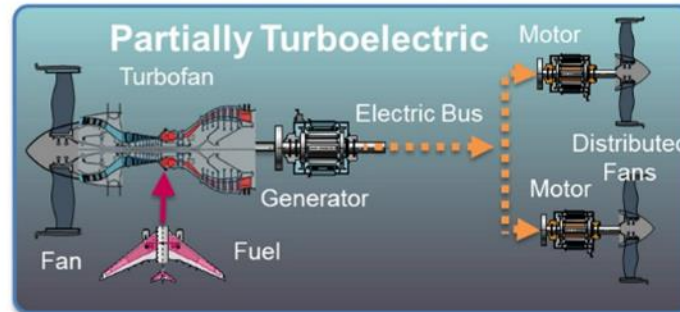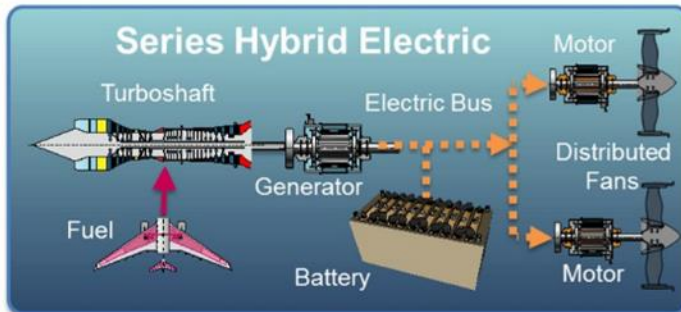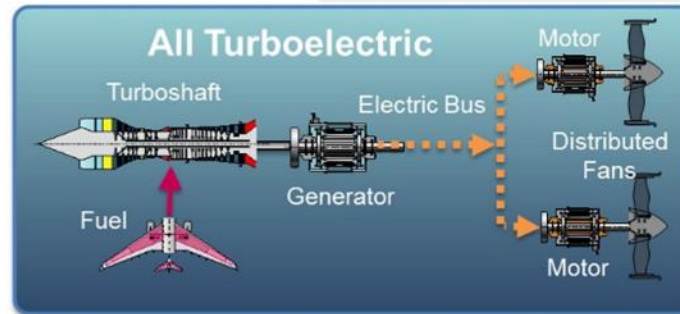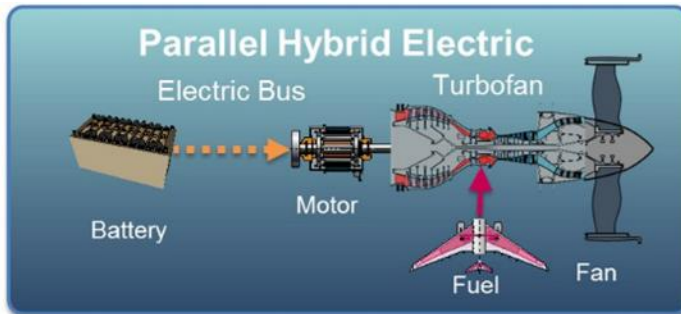


**Benefits**

– fewer emissions,

– improved fuel economy,

– quieter flight,

– improved efficiency and maneuverability,

– reduced maintenance costs, improved reliability

→ Lots of power transmission lines

3

- Lightweight, high voltage, durable, and/or high temperature insulations critically needed for future hybrid or all electric aircrafts

  - Power transmission bus, wiring, inter-connects, and electric motors (e.g., slot liner)

  - Up to 20 - 40 kV or higher
    e.g., require ~ 1 mm (40 mil) thick SOA Teflon-Kapton-Teflon (TKT)

  - 0.25 to 30 MW or higher
    Or 10 -13 kW/kg SP motor

  - DC and/or AC, 400 – 4000 Hz

  - 50 – 500 amps or higher

  - 180 – 240 ºC or higher

  - Corona PD resistant

- Current HV cable technologies not suitable for such high altitude airplane operations particularly due to corona PD contributors



4
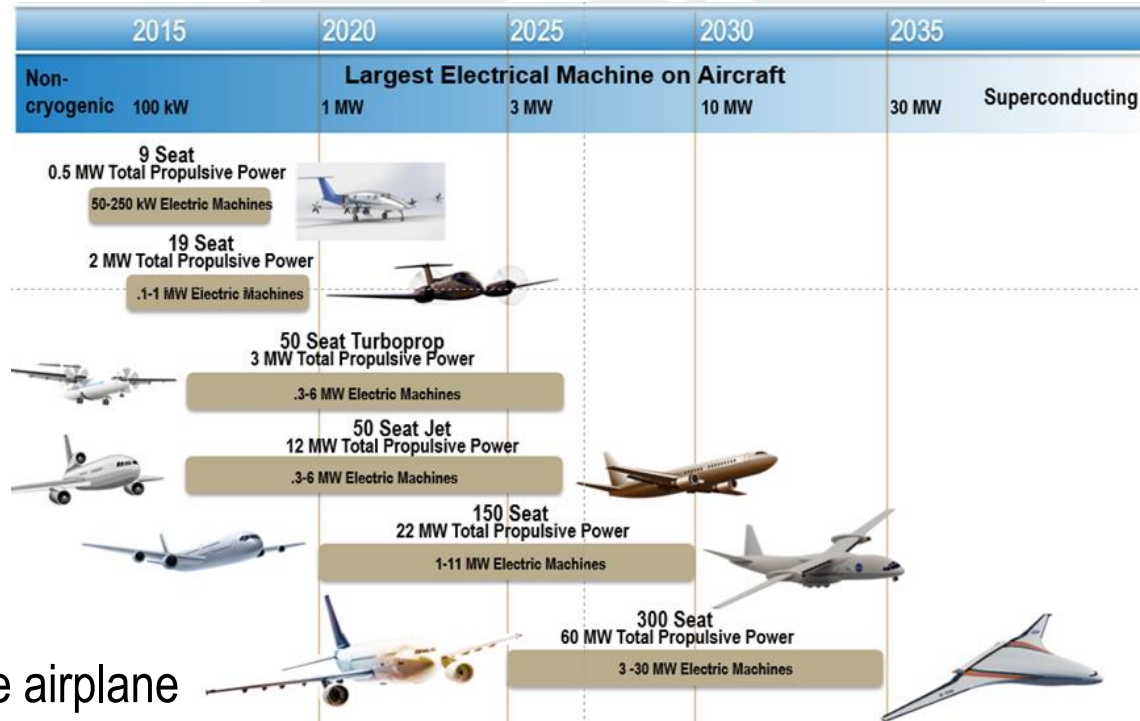
Initial Materials Efforts in High Voltage Hybrid Electric Propulsion (HVHEP) project under the NASA's Convergent Aeronautics Solutions (CAS) program (June 2015 – Sept 2017)



Legend:
- High thermal conductivity heat spreader (up to 1500 W/mK in-plane) to dissipate heat away
- Ceramic layer with high dielectric strength for electrical insulation
- Fiberglass cloth, as additional insulation, also as a stress relief
- High temperature, high thermal conductivity dielectric polymer film with self-healing capability, as a backup insulation and outer packaging
- Glass fiber reinforced epoxy composite as a supporting/load bearing structure
- Thermally conductive, low density, metal(Ni)-plated graphite foam blocks (~ 100 W/mK) with vent holes, as a heat exchanger
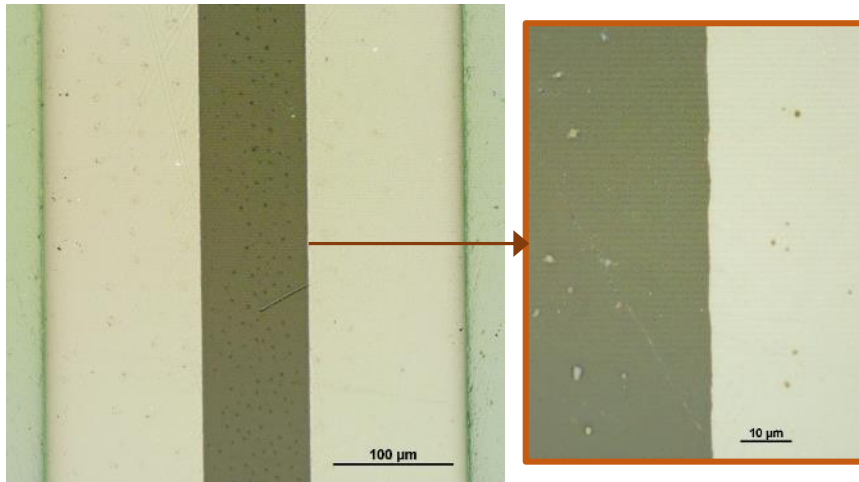- High thermal conductivity graphite cement

- Original design concept of new insulation structure, so-called multilayer functional insulation system (MFIS), on a flat conductor such as a power transmission bus bar
- Various material types with different functionalities, particularly for dielectric strength and thermal management. Heat dissipation may need for local environment, e.g., generators (~400 °C)
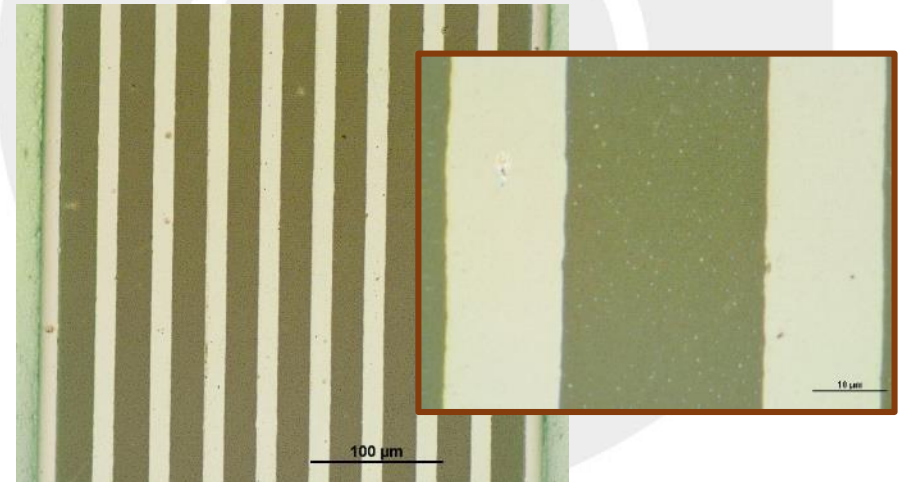
5

➢ New multilayer structures, namely  Micro-multilayer Multifunctional Electrical Insulation (MMEI) system, of well-known polymer insulation films, e.g., Kapton PI and PFA as bond layer, significantly improved dielectric breakdown voltage ($V_B$), if well-bonded.

5*KBF/5*PFA/5*KBF: 3-layers/0.38 mm th, $V_B$=38 kV          [0.5*HPP/1*PFA]$_9$ /0.5*HPP: 19-layers/0.38 mm th, $V_B$=46 kV



• Kapton PI film alone, 0.38 mm thick, $V_B$=29 kV

6

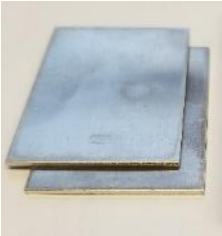Under the NASA's Transformational Tools and Technology (TTT) program (Oct 2017 -    )
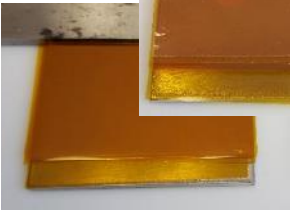
- To maximize dielectric performance of the new MMEI structures via material-design-process optimizations

- To incorporate multifunctionalities, such as high partial discharge resistance, improved durability, EMI shielding, and high thermal dissipation

- To demonstrate scale-up and commercial applicability of MMEI system

## Initial Candidate Materials, all commercially available

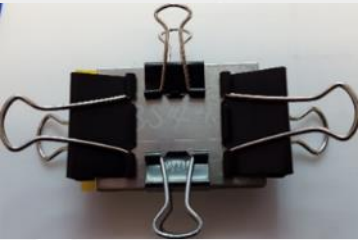- 1, 2, and 5 mil thick Thermalimide Kapton bagging film (KBF) from Airtech International, Inc. as the baseline PI

- Kapton® PI films from DuPont
  - 0.3, 1, 5 mil thick HN, a tough, aromatic film: 30HN, 100HN, 500HN, respectively
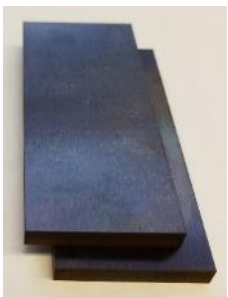  - 50HPP-ST, 0.5 mil thick with superior dimensional stability and adhesion characteristics
  - 100CRC, 1 mil thick, corona resistant films

- PFA films: 0.5 and 1 mil films from Chemours; 2 and 5 mil films from McMaster-Carr

- 2 mil thick virgin Teflon® PTFE films from McMaster-Carr

- 2 mil thick PET, Mylar A polyester films from Tekra

- 2 mil thick thermally conductive PI (TCPI) films from McMaster-Carr

- 1 mil thick electrically conductive PI (ECPI) films from McMaster-Carr

- 1.5 mil thick eGRAF® Spreadershield™ SS1500 flexible graphite from GrafTech

# Experimental: Fabrication of Dielectric Strength Test Samples



Constituent films, cleaned with alcohol and air dried

**Sample Batch #1**

1/16" thick aluminum sheets

Laid up (2 × 1.25"); PI vs PFA for skin layers

Heated in oven under compression w binder clips

Consolidated coupon for 2 test samples

**Sample Batch #2**

3/16" thick A2 tool steel

Laid up (3 × 1.25")

Heated in oven under compression w HT sealing clips

Consolidated coupon for 3 test samples

## Optimized heat fuse-bonding conditions:

- PFA:  heat to 350 ºC, dwell for 10 min (allowed to 353 ºC)

- PET:  heat to 270 °C, dwell for 10 min

  under uniform compression loading of about 8 to 8.4 psi using either 14 clips# on 2 × 1.25 inch coupon or 20 clips# on 3 × 1.25 inch coupon

  # Inconel high temperature sealing clip: rated to 370 °C, 1.5 lbs clamping force per clip

Commercial test rig, Model DT2-60-20-SR-P-C by Sefelec Eaton, France, used for material screening
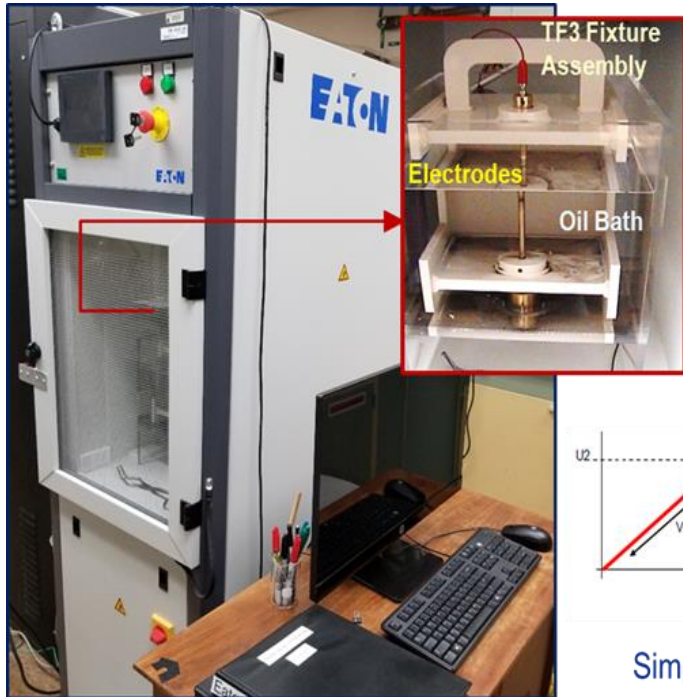


## Electrical Characteristics

|  |  | AC | DC |
|---|---|---|---|
| Output voltage: | Max | 60.0 | 84.4 |
| kV | Min | 1.8 | 2.6 |
|  | Regulation ± | 0.4 | 0.6 |
|  | Resolution | 0.017 | 0.024 |
| Ramp Rate, kV/s | Max | 5.5 | 7.8 |
| (Average speed) | Min | 0.6 | 0.5 |

Simple Ramp

Ramp by Steps
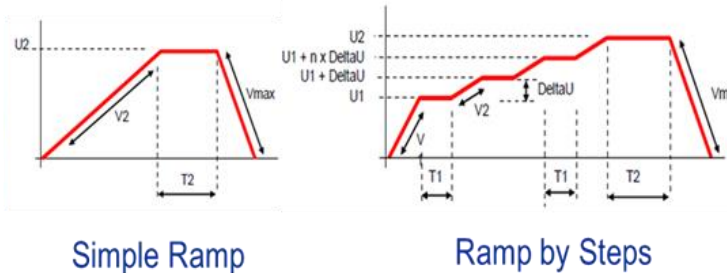
## Standardized Test Conditions

• TF3 fixture (0.25" dia. electrodes with edges rounded to 0.0313" R)

• Oil bath with PM-125 phenylmethylsiloxane

• Simple AC ramp at 0.6 kV/s

• Run reference samples with known $V_B$ before and after every actual sample group

# Results & Discussions:  Status of Invention

## Overall dielectric performance of MMEI structures

**Highest increase: ~ 61%**
→ **86.3% thickness reduction**

$y = 7.5738\ln(x) + 35.979$

$y = 41.635x^{0.467}$

**Thickness limit, ~ 0.15**

typical TKT range

× **GRC in-house test results + literature values up to 0.76 mm thick**

Legend:
- □ PI-PFA MMEI Batch #1
- ■ PI-PFA MMEI Batch #2
- × Kapton PI films
- + PFA film
- ◇ PI-PET MMEI Batch #1
- – PET film

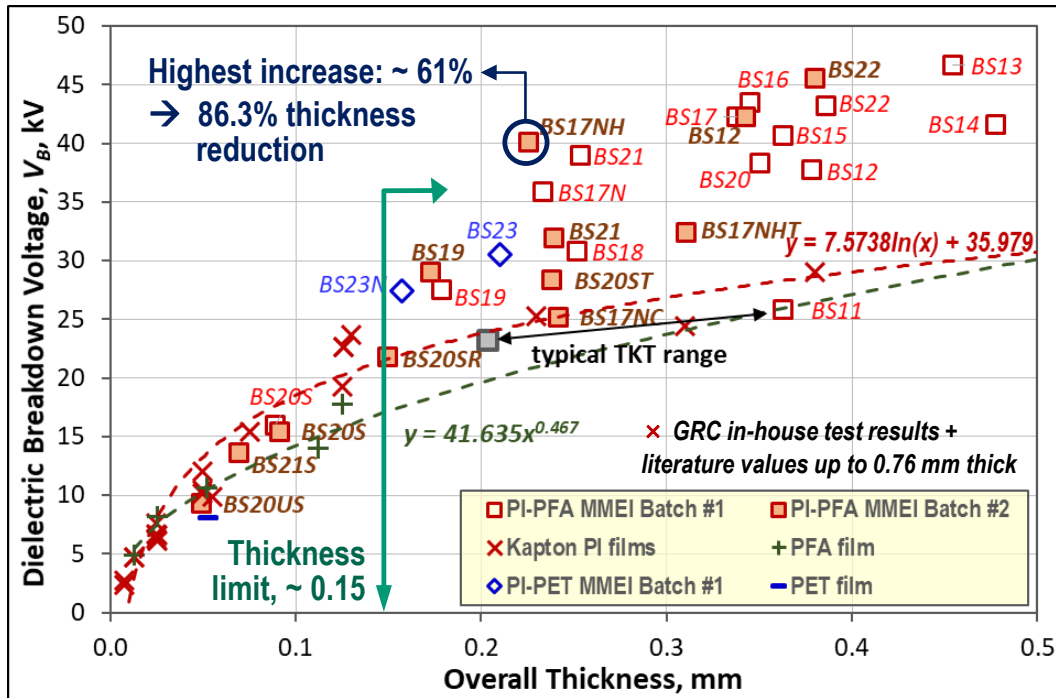(Scatter plot: Dielectric Breakdown Voltage, $V_B$, kV vs. Overall Thickness, mm. Data points labeled: BS16, BS22, BS13, BS17, BS22, BS17NH, BS12, BS15, BS14, BS21, BS20, BS12, BS17N, BS23, BS21, BS18, BS19, BS17NHT, BS23N, BS20ST, BS19, BS17NC, BS11, BS20SR, BS20S, BS20S, BS21S, BS20US)

| | Coupon ID | Layer Configuration | Overall Thickness | | |
|---|---|---|---|---|---|
| | | | Design | | Proc'ed |
| | | | mil | mm | mm |
| Batch #1 | BS11 | 5*PFA/5*KBF/5*PFA | 15 | 0.381 | 0.363 |
| | BS12 | 5*KBF/5*PFA/5*KBF | 15 | 0.381 | 0.378 |
| | BS13 | 2*PFA/5*KBF/5*PFA/5*KBF/2*PFA | 19 | 0.483 | 0.455 |
| | BS14 | 5*KBF/5*PFA/1*KBF/5*PFA/5*KBF | 21 | 0.533 | 0.478 |
| | BS15 | [2*PFA/2*KBF]₃/2*PFA | 14 | 0.356 | 0.363 |
| | BS16 | 1*KBF/2*PFA/2*KBF/5*PFA/2*KBF/2*PFA/1*KBF | 15 | 0.381 | 0.345 |
| | BS17 | [1*KBF/2*PFA]₄/1*KBF | 13 | 0.330 | 0.338 |
| | BS17N | [1*KBF/1*PFA]₄/1*KBF | 9 | 0.229 | 0.233 |
| | BS18 | [0.5*PFA/1*KBF]₆/0.5*PFA | 9.5 | 0.241 | 0.252 |
| | BS19 | [1*KBF/0.5*PFA]₄/1*KBF | 7 | 0.178 | 0.178 |
| | BS20 | [0.3*HN/0.5*PFA]₁₆/0.3*HN | 13.1 | 0.333 | 0.350 |
| | BS20S | [0.3*HN/0.5*PFA]₄/0.3*HN | 3.5 | 0.089 | 0.089 |
| | BS21 | [0.5*HPP/0.5*PFA]₉/0.5*HPP | 9.5 | 0.241 | 0.254 |
| | BS22 | [0.5*HPP/1*PFA]₉/0.5*HPP | 14 | 0.356 | 0.386 |
| | BS23N | [1*KBF/2*PET]₄/1*KBF | 13 | 0.330 | 0.158 |
| | BS23 | [1*KBF/2*PET]₄/1*KBF | 13 | 0.330 | 0.210 |
| Batch #2 | BS12 | 5*KBF/5*PFA/5*KBF | 15 | 0.381 | 0.343 |
| | BS17NH | [1*HN/ 1*PFA]₄/1*HN | 9 | 0.229 | 0.225 |
| | BS17NC | [1*CRC/ 1*PFA]₄/1*CRC | 9 | 0.229 | 0.242 |
| | BS17NHT | 2*PTFE/1*PFA/[1*HN/ 1*PFA]₄/1*HN | 12 | 0.305 | 0.310 |
| | BS19 | [1*KBF/0.5*PFA]₄/1*KBF | 7 | 0.178 | 0.173 |
| | BS20S | [0.3*HN/0.5*PFA]₄/0.3*HN | 3.5 | 0.089 | 0.092 |
| | BS20SR | [0.3*HN/1*PFA]₄/0.3*HN | 5.5 | 0.140 | 0.149 |
| | BS20ST | [0.3*HN/2*PFA]₄/0.3*HN | 9.5 | 0.241 | 0.238 |
| | BS20US | [0.3*HN/0.5*PFA]₂/0.3*HN | 1.9 | 0.048 | 0.049 |
| | BS21 | [0.5*HPP/0.5*PFA]₉/0.5*HPP | 9.5 | 0.241 | 0.239 |
| | BS21S | [0.5*HPP/0.5*PFA]₂/0.5*HPP | 2.5 | 0.064 | 0.069 |
| | BS22 | [0.5*HPP/1*PFA]₉/0.5*HPP | 14 | 0.356 | 0.380 |

* indicated thickness in mil (1/1000 inch)
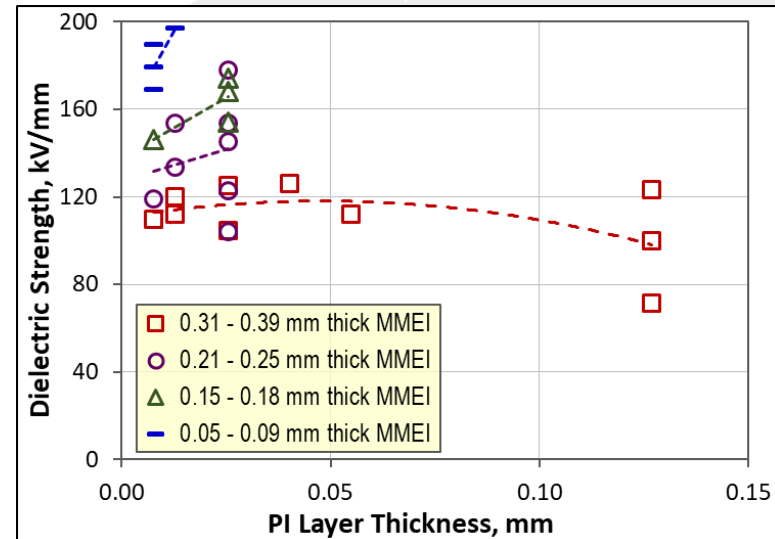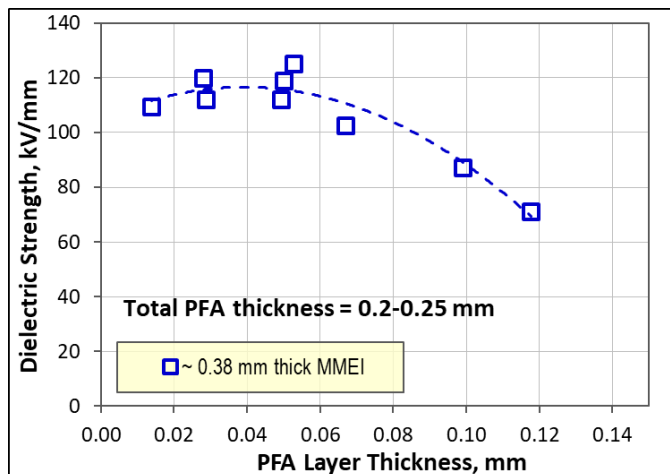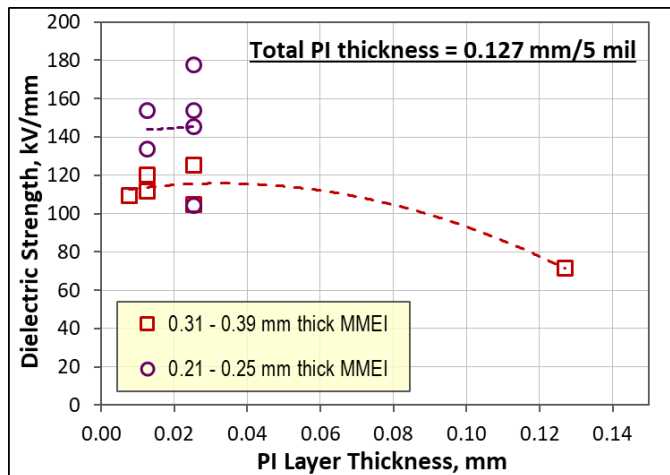
• Parameters that control $V_B$ or $K$ of MMEI:  <u>total thickness</u>, <u>individual layer thickness</u>, <u>total accumulated thicknesses of constituent materials</u>, <u>overall thickness ratio of constituent materials</u>, and <u>total number of layers or interfaces</u> in addition to <u>bonding integrity</u>.

# Results & Discussions:  Status of Invention

## Effects of individual layer thickness



- For both PI and PFA, $K$ of MMEI structures increased with decreasing layer thickness, but leveled off at ~ 0.05 mm which seemed to be related to the overall thickness limit.

- Both PI and PFA contributed to the overall performance of MMEI structures.

13

## Effects of total constituent material thickness
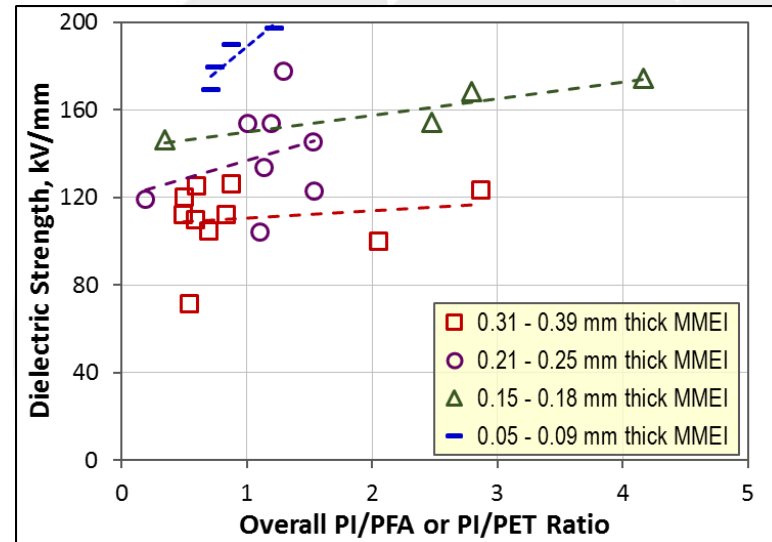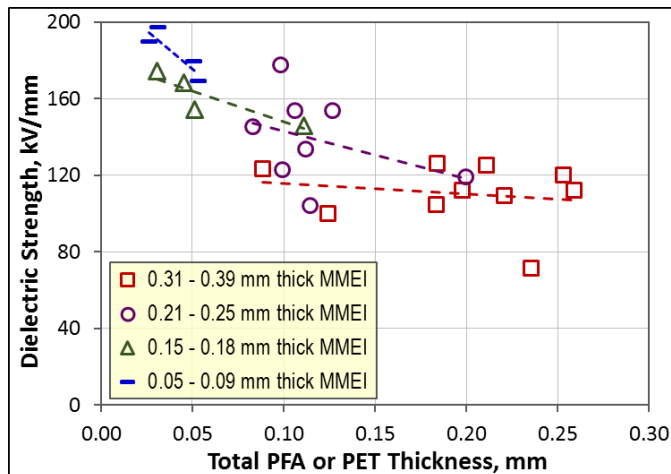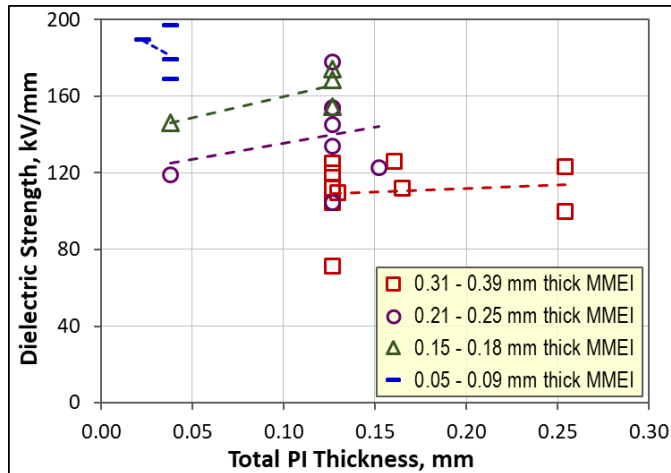


- In general, *K* of MMEI structures increased with increasing total thickness of PI layers, but decreased with increasing that of PFA or PET layers.

- Contribution of PI layers on the overall *K* of MMEI structures was greater than that of PFA or PET bond layers.
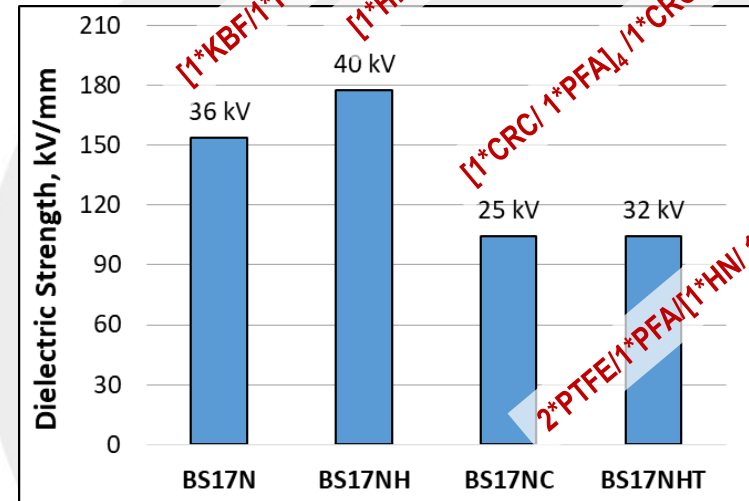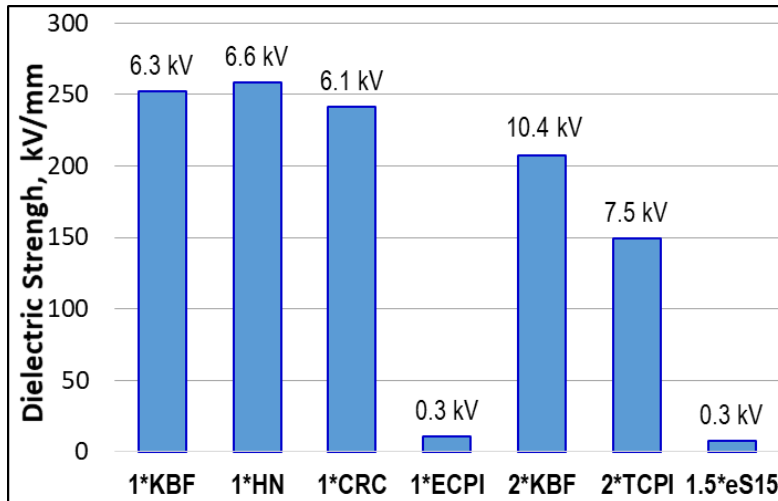
## Effects of total number of layers or interface
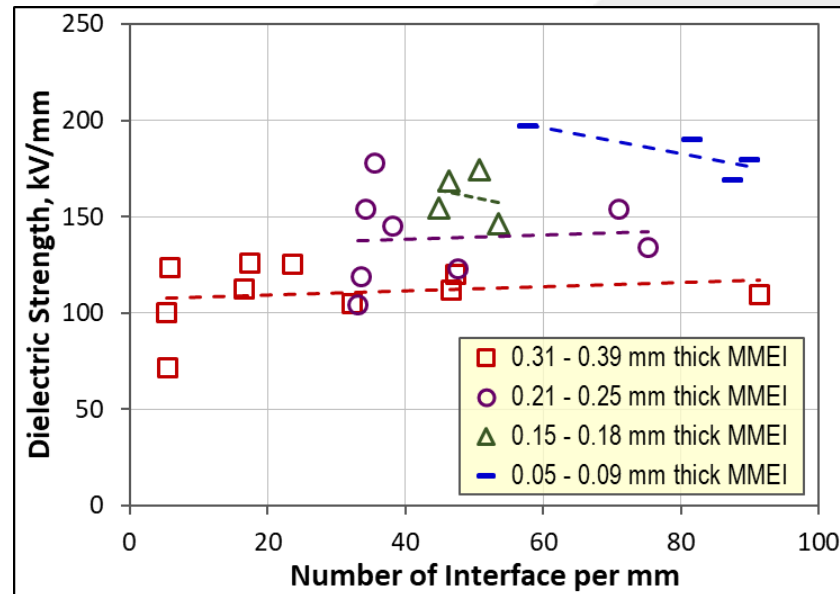


- *K* of MMEI structures increased slightly with increasing number of interface or total number of layers, but decreased when their overall thickness was less than ~ 0.18 mm, which seemed to be related to the overall thickness limit on the MMEI effectiveness.

## Effects of PI material modifications



- Various types of PI considered for multifunctionalities of MMEI
- Modifications, typically via addition of fillers or additives, decreased $K$ of either PI alone film or MMEI structures.  Much worse in MMEI structures, especially for the corona resistant CRC PI film
- Unexpected drop of $K$ by adding 2 mil thick PTFE layer in BS17NHT, possibly due to weaker bonding between PFA and PTFE?

→ Results of all those semi-quantitative analyses are systematically applied to design future, more efficient MMEI structures with maximized $V_B$ or $K$.

16

## Typical dielectric breakdown failure modes



PFA

(a) 100 μm  (b) 100 μm  (c) 100 μm  (d) 100 μm

(a)  0.013 mm thick
(b)  0.025 mm thick
(c)  0.05 mm thick
(d)  0.125 mm thick;
All showed melt, char, THP (Thru-hole perforation) or PP (partial perforation).

Kapton PI

(a) HPP-ST 100 μm  (b) HN 100 μm  (c) KBF 100 μm  (d) HN 1.5 mm

DZW

(a)  0.013 mm th.;  char, THP
(b)  0.025 mm th.; cracks, char, THP
(c)  0.05 mm th.; cracks, cavitation, melt, char, PP
(d)  0.126 mm th.; extensive cracks-cavitation, melt, char, PP

- The hole size in PFA films increased with increasing thickness but only up to ~0.025 mm.

- Failure mode in PI changed with increasing thickness, i.e., melting, charring, and THP up to 0.013 mm → additional micro-cracking before THP up to 0.025 mm → PP at and above ~0.05 mm.

- Note that DZW in (d) defined the width of damage band around the electrodes.

# Results & Discussions:  Status of Invention

## Typical dielectric breakdown failure modes



MMEI

(a) 0.05 mm th. BS20US; cracks, debond, melt, char, THP,
(b) 0.125 mm th. BS20SR,
(c) 0.173 mm th. BS19,
(d) 0.31 mm th. BS17NHT,
(e) 0.2235 mm th. BS17NH,
(f) 0.345 mm th. BS16,
(g) 0.38 mm th. BS22,
(h) 0.455 mm th. BS13;

(b) thru (h) all showing cracks, cavitation, debond, melt, char, and PP.
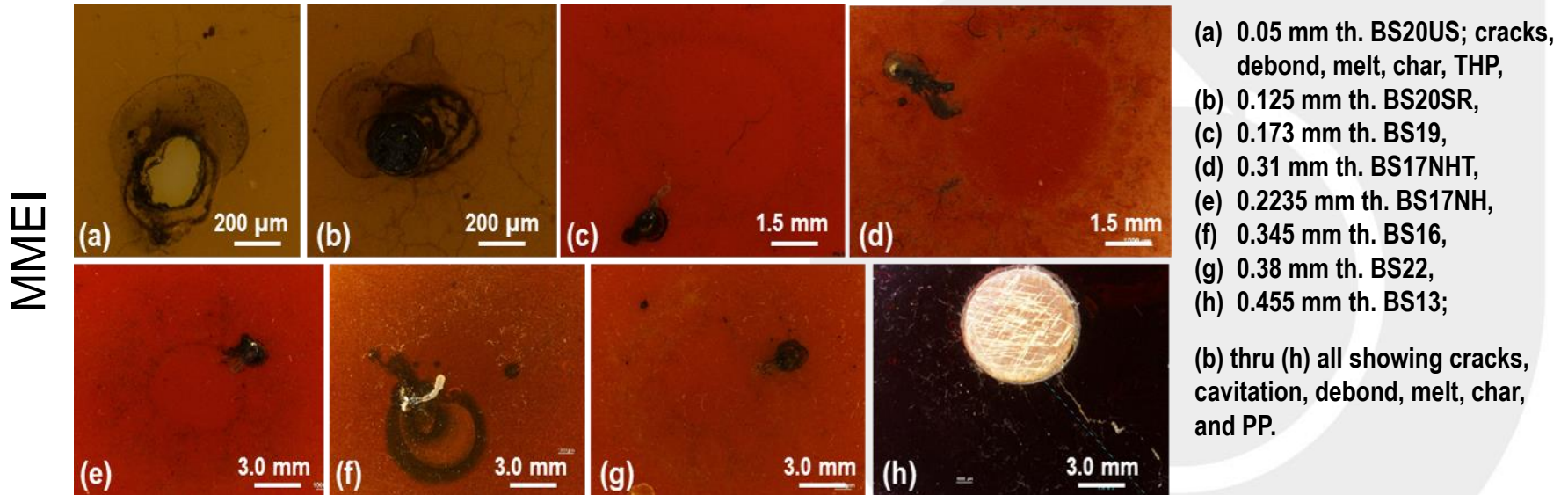
- Additional unique failure mode in MMEI structures was debonding or inter-layer separations.

- Failure mode of MMEI structures affected by (i) overall thickness, (ii) individual layer thickness, (iii) PI/BL ratio.

- Most MMEI structures involved microcracking or cracking, cavitation, debonding, melting, charring, and PP, but the ultimate breakdown occurred via the localized charring and PP.

- Samples failed by THP normally showed lower $V_B$ or $K$.

## Dielectric breakdown damage evolution in MMEI structures

BS17N; [1*KBF/1*PFA]$_4$ /1*KBF;  9-layers, 0.233 mm thick
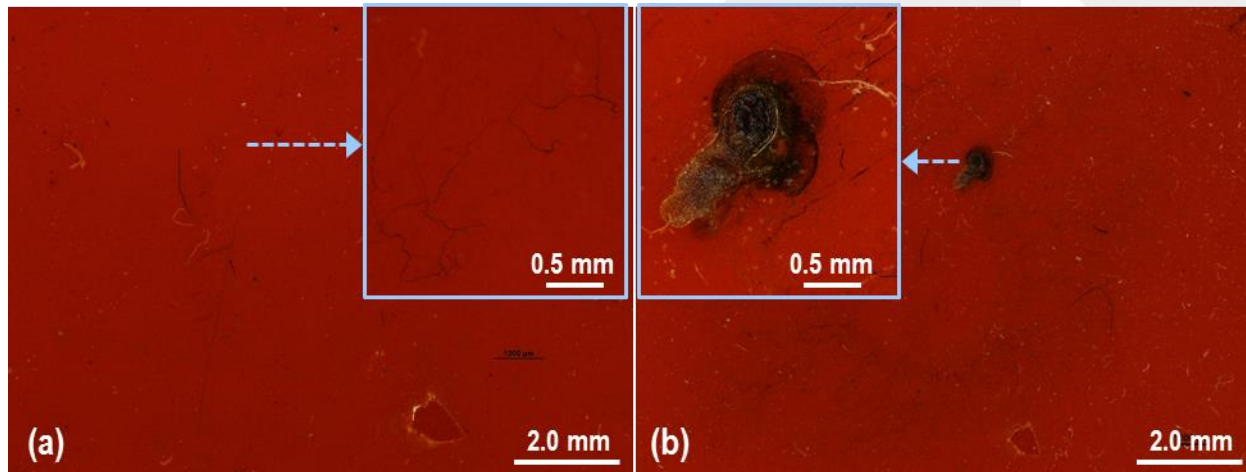


(a) Micro-cracking, cavitation, presumably in Kapton PI layers at 22 kV

(b) Extensive crack propagation, cavitation, localized debonding, melting, charring, and PP at dielectric breakdown at 36 kV

- Damage evolution sequence in MMEI structures was determined experimentally as a function of V.
- From the extensive failure mode analyses, for a given overall thickness, the failure mode transitioned from more catastrophic mode involving cracking, cavitation, charring, THP in single polymer insulation films to more gradual or progressive mode involving microcracking, cavitation, melting, channeling, debonding, interfacial swelling, charring and PP in the new MMEI structures.

19

# Results & Discussions:  Status of Invention

## *K* and DZW correlation in MMEI structures
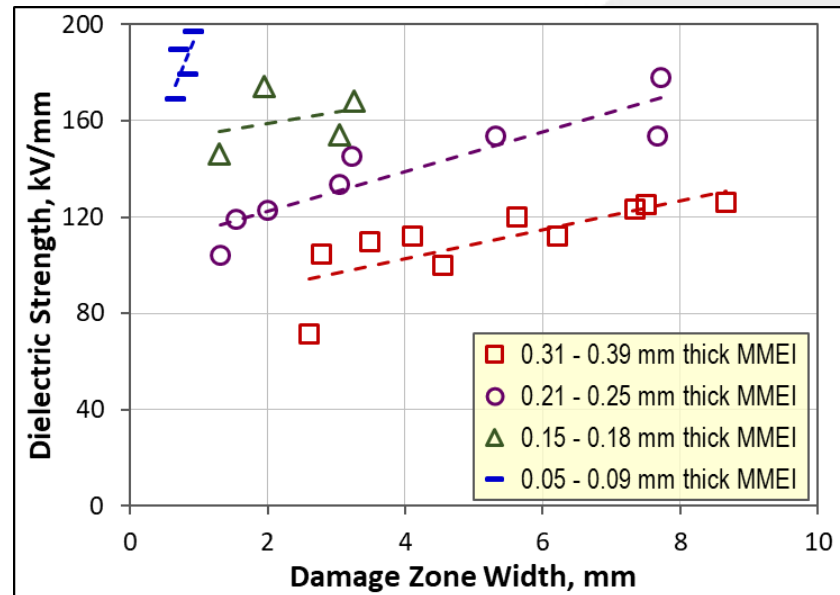


- In MMEI structures, the higher *K* was, the larger DZW was or vice versa regardless of overall thickness.

- Dielectric breakdown failure of MMEI structures proceeded with a progressive damage evolution involving more damage types/events and larger damage zones, i.e., more energy involved in the breakdown process → the higher dielectric strength.

# Results & Discussions:  Design and Process Optimizations
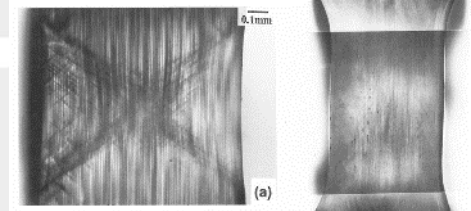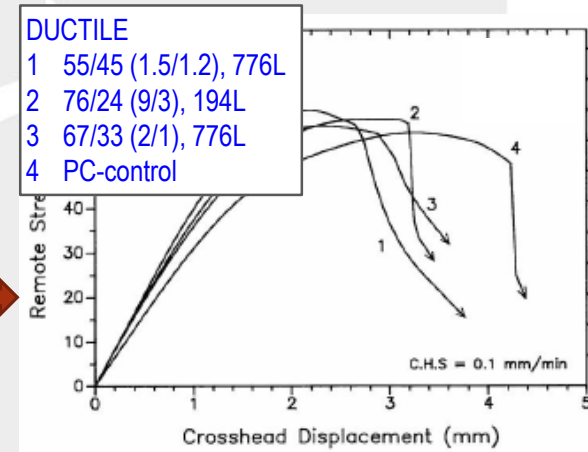
## Example of optimum MMEI design
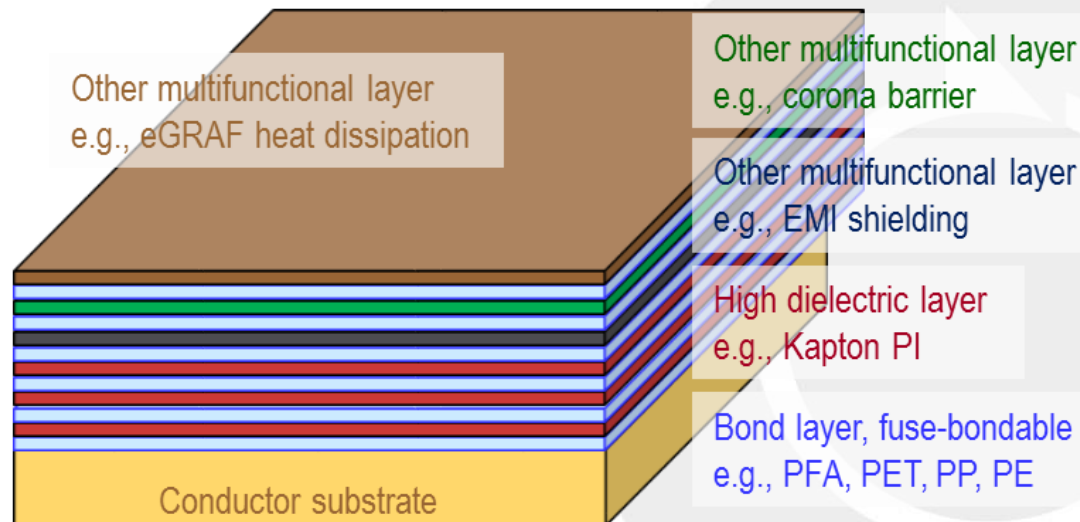


- In spite of significant performance improvement of the MMEI structures to date,  their performance can be further improved when their design-structural configurations, insulation material types, and process-fabrication conditions are optimized.

- MMEI structures can incorporate multifunctionalities by the nature of their design capabilities, such as Corona PD resistance, EMI shielding, mechanical durability, or thermal management, etc.

# Results & Discussions:  Design and Process Optimizations

Potential evidence of improved structural durability

**PC/San v% (layer thickness, μm), # of layers**



BRITTLE
1  SAN-control
2  30/70 (4/8), 194L
3  25/75 (11/34), 49L
4  53/47 (23/22), 49L

SEMI-BRITTLE
1  65/35 (27/15), 49L
2  45/55 (4.9/5.4), 194L
3  40/60 (1.3/2), 776L
4  74/26 (33/13), 49L
5  53/47 (3.6/3.3), 388L

DUCTILE
1  55/45 (1.5/1.2), 776L
2  76/24 (9/3), 194L
3  67/33 (2/1), 776L
4  PC-control
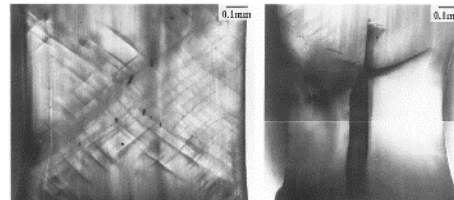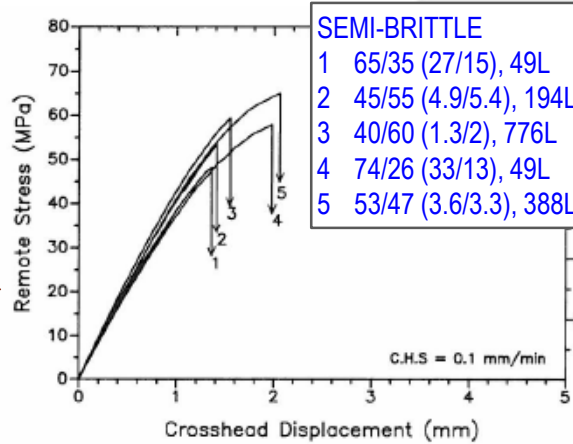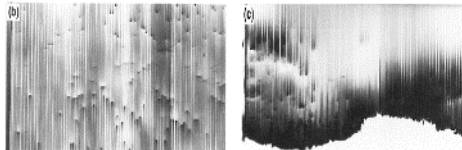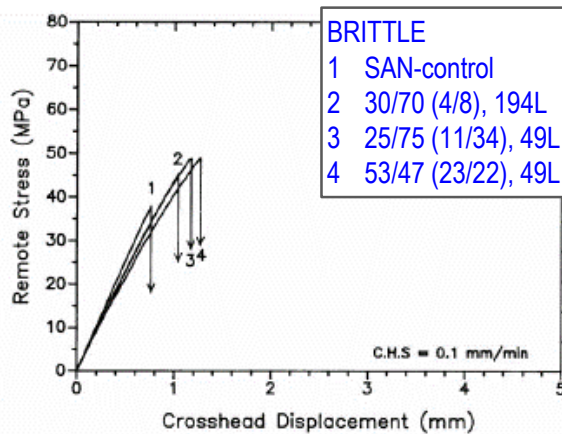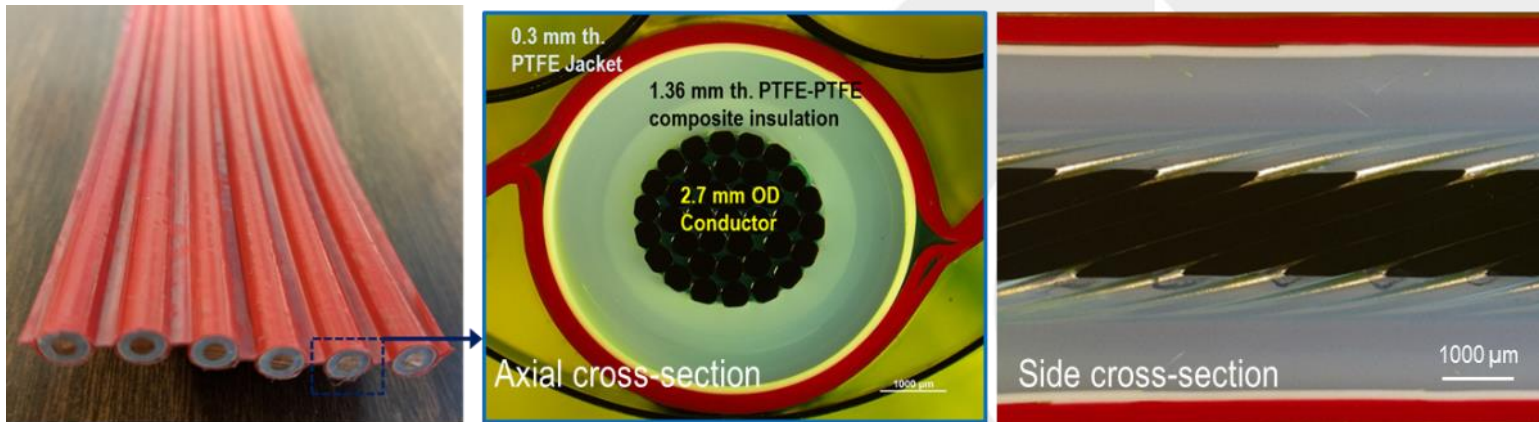
- Brittle to ductile transition occurred with increasing PC v% or decreasing layer thickness in PC/SAN multilayer structures.

- Ref: E.E. Shin, A. Hiltner, and E. Baer, "The Brittle-to-Ductile Transition in Microlayer Composites", J. of Applied Polymer Science, 47,  p269, 1993.

# Results & Discussions: Commercial Benefit/Applicability

## HV Power Pod Cable by GORE



- Unique design developed to carry 0.25 MW at 15 kV (but rated to 40 kV), and applicable to -80 C to >260 ℃ use temperature

- Consisted of six identical conductor pods insulated by the GORE's proprietary PTFE-PTFE composite and arranged horizontally by a corona resistant PTFE jacket

- By GORE's standard testing, $V_B$ of the PTFE-PTFE composite insulation was ~ 39 kV, but it dropped to ~ 29 kV when the PTFE jacket was added. The cause not fully identified.

HV Power Pod Cable by GORE:  $V_B$ and failure mode measurement at GRC



- The optimized bend configuration produced reproducible $V_B$, 30.2±1.7 kV, consistent with the GORE data.
- $V_B$ of the cable after removing jacket was also 29.9±0.04 kV, which suggested that the jacketing process at GORE seemed to cause permanent change in the main PTFE composite insulation.
- 600V silicone hookup wire performed exceptionally well, reached 23.9 kV breakdown voltage.
- Determination of Inter-conductor $V_B$ was not successful for the GORE cable.

# Results & Discussions:  Commercial Benefit/Applicability

HV Power Pod Cable by GORE:  Design options to apply MMEI
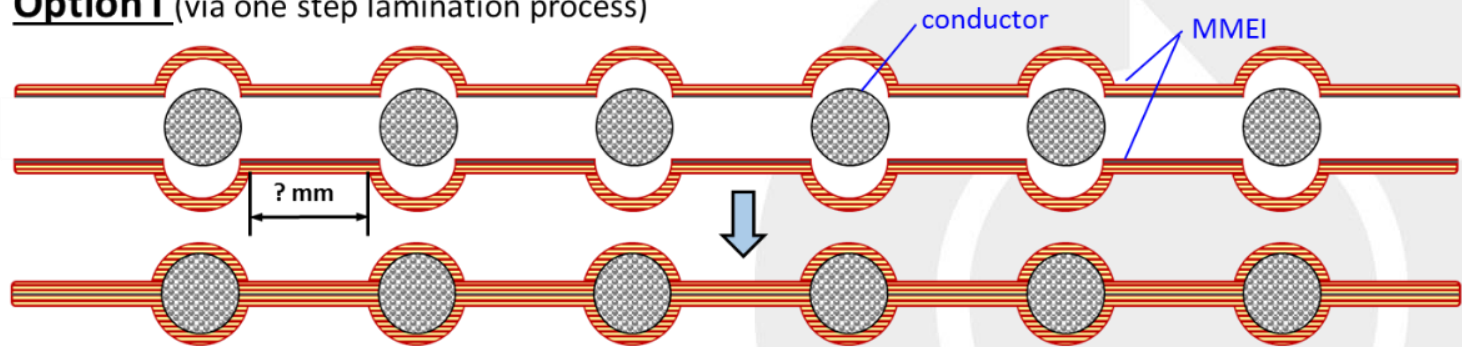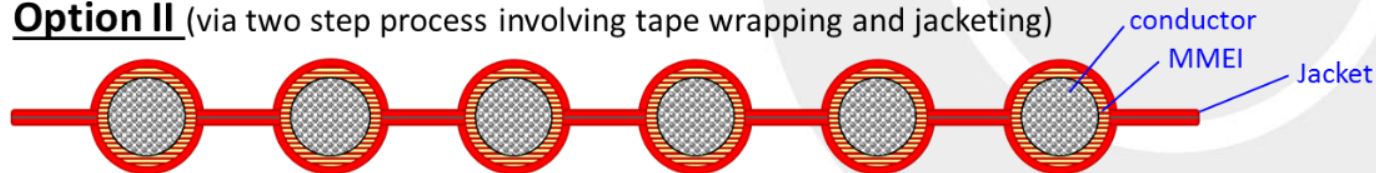


- Either a modified BS22 ($[0.5*HPP/1*PFA]_9$ /0.5*HPP, 0.38 mm th) or BS17NH ($[1*HN/1*PFA]_4$ /1*HN, 0.225 mm th) MMEI configuration was considered.

- Option II: ideally more solid insulation VS. Option I: simpler & easier to process, e.g., vacuum-bagging/autoclaving

- Overwrap seamlines in option II can be a weak spot for high voltage due to trapped air.

# Results & Discussions:  Commercial Benefit/Applicability

HV Power Pod Cable by GORE:  Design optimization of Option I



**Design of Test Coupons/Samples**

**Dielectric strength testing**
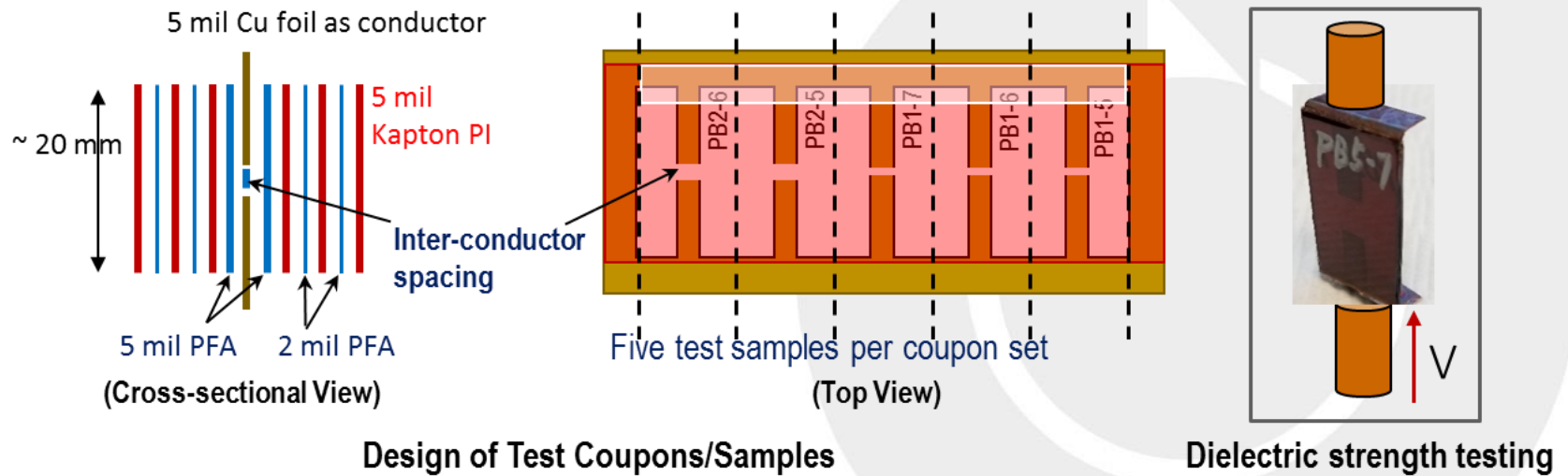
- Experimental determination of web width (= inter-conductor spacing - 2 × MMEI thickness) via measurement of $V_B$ through PFA bondline or PFA-PI interface

- Four different inter-conductor spacing tested: 1, 2, 3, and 5 mm;  4 repeats per spacing

- Successful dielectric strength testing in the GRC test rig → Failure mode analysis

HV Power Pod Cable by GORE:  Design optimization of Option I



**PB5-7, 5 mm spacing:** melt, cavitation, & possible perforation on PFA; PFA-PI interface debond
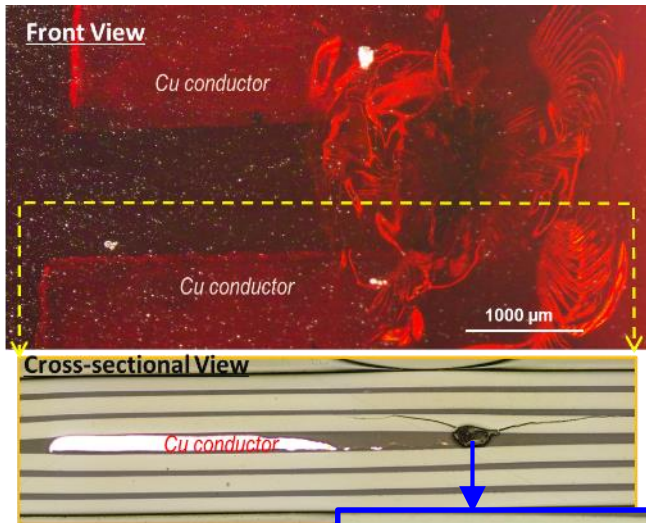
**PB1-5, 1 mm spacing:** melt, cavitation, possible perforation on PFA, PFA-PI interface debond, cracks on PI
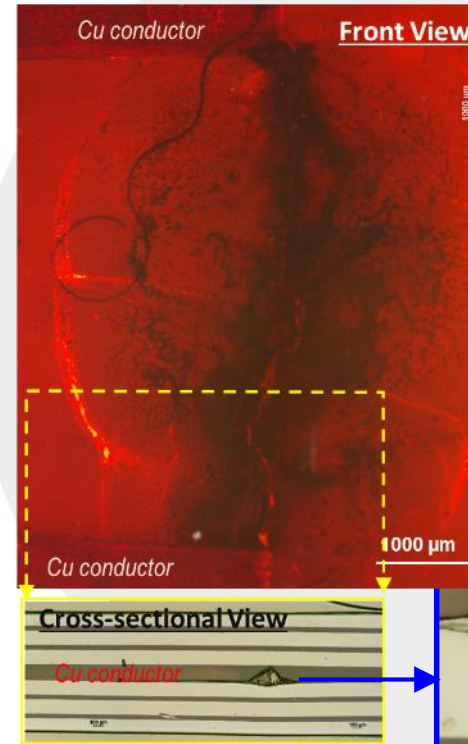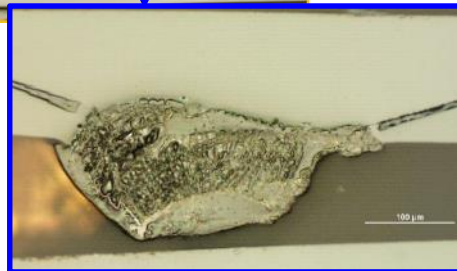
- Validation of failure path through PFA bondline or PI-PFA interface, thus validated test results

## HV Power Pod Cable by GORE:  Design optimization of Option I



$y = 41.687x^{0.4676}$

$y = 23.894x^{0.4019}$

Legend: □ Thru Thickness  △ Thru Bondline

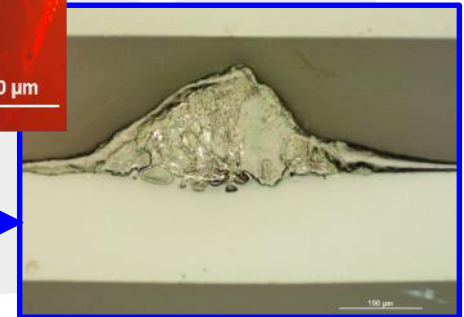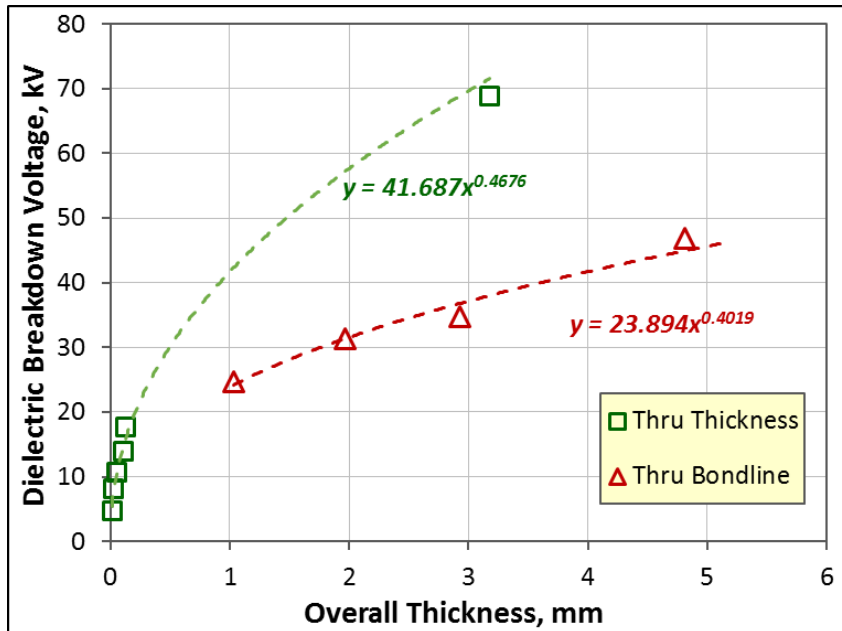| Flat cable with 6 high voltage conductors   AWG 4 equivalent | | GORE | | MMEI Option I | | MMEI Option II | |
|---|---|---|---|---|---|---|---|
| | | TH, mm | OD, mm | TH, mm | OD, mm | TH, mm | OD, mm |
| Conductor: | AWG 10 (37/0.404mm), Ni plated copper | | 2.70 | | 2.70 | | 2.70 |
| Insulation: | PTFE-PTFE Composite | 1.34 | 5.38 | | | | |
| | MMEI: modified BS22 | | | 0.394 | 3.49 | | |
| | MMEI: modified BS22 | | | | | 0.381 | 3.46 |
| Jacket: | PTFE, Corona resistant | 0.3 | 5.98 | | | | |
| | 5 mil PFA + 5 mil PTFE | | | | | 0.254 | 3.97 |
| Web width: | | 2 | | 4.2 | | 3 | |
| Web thickness: | | 0.6 | | 0.787 | | 0.508 | |
| Final Cable | | | 5.98 | | 3.49 | | 3.97 |
| Overall width, mm | | | 53.5 | | 51.2 | | 41.8 |

- 5 mm spacing selected for the 40 kV requirement including a safety factor consideration
- Final OD of option I or II cable may vary depending on modification of MMEI configuration to incorporate other multifunctionalities, but yet significantly thinner than that of GORE cable
- Initially, ~ 1 m long cables to be fabricated

# Results & Discussions:  Commercial Benefit/Applicability

## HV high frequency bus bar with MERSEN



3"×1/8" Aluminum Conductor with round edges

Gap between conductors

0.3 mm th. PTFE Jacket

0.5 mm th. PTFE Insulation

0.04 mm th. Kapton Insulation

Corona barrier or EMI shielding layer
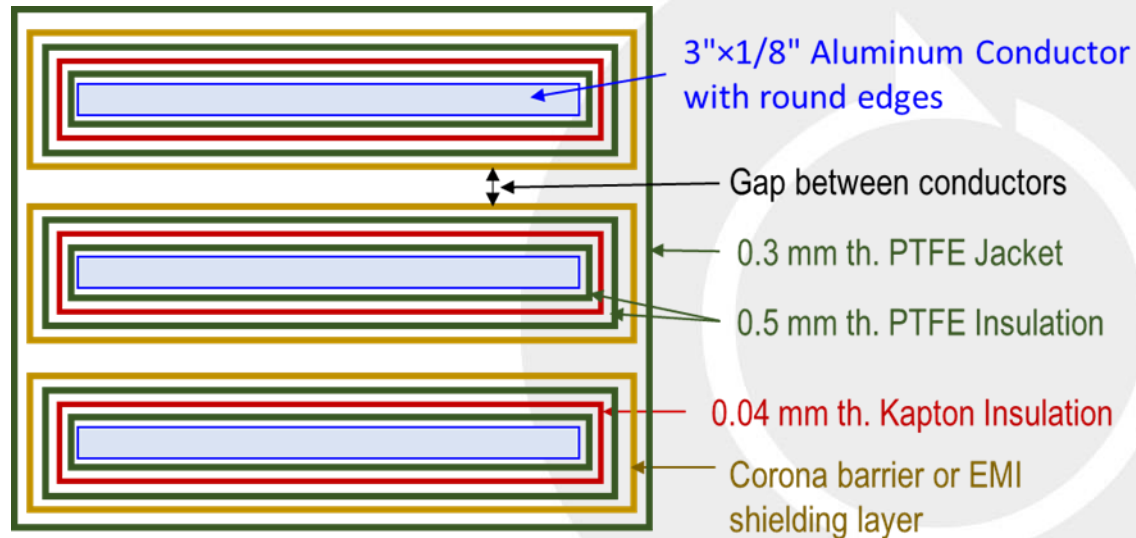
- A three-phase system for 1 MW up to 10 MW operating power with operating voltage of 20 kV ( designed for 40 kV), high frequency (400 Hz up to 4000 Hz), and temperature up to 180 ºC

- Three prototypes with three different conductor thickness, fully insulated by MERSEN

- Two sets of blank conductors to apply MMEI structures

# Summary and Conclusions

- Multilayer structures of well-known polymer insulation materials, namely MMEI, were newly developed and evaluted for HV insulation.  Based on extensive evaluations to date, key findings are as follows:

    - MMEI structures with various Kapton PI materials and PFA or PET as a bond layer achieved 61% increase in $V_B$ or $K$ compared to that of Kapton PI alone films or the SOA TKT, thus resulted in 86.3 % decrease in insulation thickness.

    - Dielectric performance of MMEI structures was governed by various material, process, and structural parameters, such as dielectric properties of constituent materials, inter-layer bonding integrity, overall thickness, total number of layers or interface, individual layer thickness, and ratio of constituent materials.

    - Good inter-layer bonding integrity was essential for improved $V_B$ or $K$.

    - $K$ of the MMEI structures increased with (i) decreasing individual layer thickness regardless of material type, (ii) increasing total accumulated thickness of PI or overall PI/BL ratio, and (iii) increasing number of interface or total number of layers, but only above the overall thickness limit of 0.15 mm.

# Summary and Conclusions, Cont'd

– Contribution of Kapton PI on overall MMEI dielectric performance was greater than that of PFA or PET, and as a bond layer PFA performed better than PET.

– For a given overall thickness, the failure mode seemed to change from more catastrophic mode involving cracking, cavitation, charring, PP or THP in single polymer insulation films to more gradual or progressive mode involving microcracking, cavitation, melting, channeling, debonding, interfacial swelling, charring and PP in the new MMEI structures.

– Dielectric breakdown failure of MMEI structures proceeded with a progressive damage evolution involving more damage types/events and larger damage zones, which suggested that more energy was involved in the breakdown process, thus resulted in the higher dielectric strength.

– Material modifications, typically via addition of fillers or additives, decreased $K$ in either PI alone film or MMEI structures since the fillers or additives, especially their interfaces with matrix material, acted as defects.

– Various responsible mechanisms for the significant property improvement of the new MMEI system were postulated, but should be validated experimentally.

–  Improvement of processing, e.g., more accurate control of fuse-bonding temp, compression loading at all temp, and cleanliness, granted additional increase of $V_B$ in various MMEI structures, but thinner structures below the limitation, 0.15 mm, was less affected.

- Design and performance evaluations of scaled-up MMEI system were initiated to validate their practicality and applicability using the SOA commercial HV power transmission systems including GORE's HV power pod cable and MERSEN's HVHF bus bar prototypes:

  –  $V_B$ of GORE cable was measured successfully using the GRC dielectric strength test rig.

  –  Two options to apply MMEI system to GORE pod cable were developed including determination of optimum dimensions, fabrication methods and procedures.

  –  With MERSEN, a meter-long 3-phase bus bar prototype has been developed for 1 MW up to 10 MW power with operating voltage of 20 kV ( designed for 40 kV), high frequency (400 Hz up to 4000 Hz), and up to 180 ºC use temp.

  –  Design and fabrication procedures for applying MMEI system to the same blank bus bar are being developed.

# Future Work Plan

The following tasks are planned to continue for development and improvement of the MMEI system:

- Material-design-process optimizations, especially for multifunctionalities including inorganics, ceramics, or metals

- Scale up and commercialization feasibility assessment

- More sophisticated performance evaluations of the MMEI structures including synergistic durability assessment

- Experimental validation of potential mechanisms on performance enhancement of MMEI structures

## Acknowledgments

- W. L. GORE & ASSOCIATES, INC., Landenberg, PA

- MERSEN New Product Development, Rochester, NY.

- Special thanks to A. Woodworth, Janet Hurst, and the rest of project team at GRC.

- This work has been sponsored by NASA's Convergent Aeronautics Solutions (CAS) program initially, and by Transformational Tools and Technology (TTT) program currently, as a part of NASA's Transformative Aeronautics Concept Program (TACP) under Aeronautics Research Mission Directorate (ARMD).

# Thank You for your attention!

## Any Questions?